Development of an aqueous two-phase emulsion using hydrophobized whey proteins and erythritol

Ashkan Madadlou, Arnaud Saint-Jalmes, Fanny Guyomarc'H, Juliane Floury, Didier Dupont

Highlights

- Whey protein isolate (WPI) was hydrophobized by acetylation and heating
- Hydrophobized WPI and alginate were immiscible and formed W/W emulsions
- Erythritol addition to the WPI improved emulsification and emulsion stability
- Erythritol induced interactions between hydrophobized protein particles
- Furthermore, it decreased the air-water surface tension of WPI solution

Development of an aqueous two-phase emulsion using hydrophobized whey proteins and erythritol

Ashkan Madadlou[1], Arnaud Saint-Jalmes[2], Fanny Guyomarc'h[1], Juliane Floury[1], Didier Dupont[1*]

[1] *STLO, UMR 1253, INRA, Agrocampus Ouest, 35000 Rennes, France*

[2] *Univ Rennes, CNRS, IPR (Institut de Physique de Rennes) - UMR 6251, F-35000 Rennes, France*

---

*Corresponding author, Email: didier.dupont@inra.fr

Abstract

Formation of aqueous two-phase (ATP) emulsions relies on the immiscibility of two (bio)polymeric phases. Herein, we report that hydrophobization of whey proteins via a pre-acetylation and succeeding acetylation/heating combined process makes solutions of whey protein isolate (WPI) immiscible with alginate solutions. Erythritol was also added at different concentrations (0, 52, 105, and 158 mg/g) into the hydrophobized WPI solution. Subsequently, emulsions at an alginate to WPI weight ratio of 0.1 to 0.9 were prepared. Erythritol supplementation facilitated emulsification and increased emulsion stability, so that at the erythritol concentration of 105 mg/g, the emulsion was stable for a minimum duration of 7 days. The droplet size evolved and reached to ≈5 μm during this period. The hydrophobized protein had a mean hydrodynamic diameter of 80 nm, ζ-potential of –39 mV, and intrinsic fluorescence emission peak of 335 nm. Erythritol addition did not influence any of the above-mentioned characteristics. However, the hydrophobized WPI solution changed from Newtonian to a more viscous and shear-thinning fluid by adding erythritol at concentrations ≥105 mg/g, due probably to the induction of interaction among protein particles. A diameter of 150 nm was calculated for the air-dried hydrophobized protein particles using atomic force microscopy images, supporting the assumption that exclusion of erythritol from the protein particles surface induced inter-particle interactions. Erythritol addition at 105 mg/g had a twofold larger influence on the surface tension of hydrophobized WPI compared to water. It decreased the surface tension of hydrophobized WPI to 45 mN/m after droplet ageing for 350 seconds.

Keywords: Emulsion; Whey protein; Water-in-water; Hydrophobicity.

1. Introduction

Aqueous two-phase (ATP) or water-in-water (W/W) emulsions consist of droplets of a macromolecularly crowded aqueous solution, phase separated within a coexisting immiscible

aqueous phase (Dewey, Strulson, Cacace, Bevilacqua, & Keating, 2014). ATP emulsions can be more biocompatible than oil-containing emulsions, because for instance the ATP emulsions do not contain synthetic surfactant. The emulsions are increasingly used for diverse objectives including bioactives delivery and synthesis of hydrogel particles (Song et al., 2016). Recently, carboxymethyl cellulose droplets dispersed within a gelatin solution were used for encapsulation of probiotic bacteria (Singh, Medronho, Miguel, & Esquena, 2018).

Thermodynamic incompatibility between two hydrophilic non-oppositely charged polymers which causes immiscibility and segregative micro-phase separation (Esquena, 2016) is a prerequisite to form ATP emulsions. It depends on variables such as pH value, ionic strength (Grinberg & Tolstoguzov, 1997; Moschakis, Chantzos, Biliaderis and Dickinson, 2018) and the difference between the hydrophilicity of the (bio)polymers (Grinberg & Tolstoguzov, 1997). The main drawback of ATP emulsions is their extremely low stability; the droplets rapidly coalesce and the emulsion breaks down to macroscopically separated two layers (Esquena, 2016). Stabilization of ATP emulsions is conventionally achieved through emulsion gelation, so that the phase separation kinetics is arrested thanks to a fast gelation rate of the continuous phase. Gelator precursors can be introduced into two immiscible polymeric solutions to cause gelation when the solutions get in contact by mixing (Mytnyk et al., 2017). Alternatively, interfacial accumulation of colloidal particles is used to stabilize water-in-water emulsions without gelling the continuous phase (Nicolai & Murray, 2017). In this approach, particles are added into the mixture of two incompatible polymer components (Poortinga, 2008), partially partitioned into both phases (de Freitas, Nicolai, Chassenieux, and Benyahia, 2016). Due to osmotic repulsion by both polymers, the particles are depleted from the aqueous phases towards the interfacial boundary (Firoozmand, Murray, & Dickinson, 2009). Different types of particles including fat, latex, protein, liposomes, mineral platelets, cellulose nanocrystals, and bacteria have been utilized for stabilization of ATP emulsions

(Ganley, Ryan, & van Duijneveldt, 2017). Finally, it is possible to enhance stability of ATP emulsions by increasing the incompatibility between the two phases by varying the hydrophilicities of the macromolecules and/or the quality of the aqueous solvent (Walstra, 2003). Modification of the chemical structure of proteins can influences their hydrophilicity (Tyagi & Gupta, 1998) and allow to form ATP emulsions.

Chemical modification of proteins due to the wide array of available functional groups is easy to perform and fascinating. It allows creating therapeutic conjugates and generating novel constructs (Spicer & Davis, 2014). Recently, we hydrophobized whey proteins, a family of food-grade and commercially available globular proteins, through a procedure that consisted of pre-acetylation and subsequent acetylation/heating combined process (Madadlou, Floury, Dupont, 2018). Herein, we report the applicability of the acetylated (hydrophobized) whey proteins to form alginate-in-protein ATP emulsions. In such conditions, non-hydrophobized whey proteins including native and heat-treated WPI (whey protein isolate) samples were miscible with alginate. Besides, the solvent quality of the continuous phase of the emulsion was modified to improve the emulsification process and increase the stability of the ATP emulsion.

Polyols (including sugar alcohols) are known to change the solvent properties of water and enhance hydrophobic interactions of proteins (Gekko, 1981; Cioci, 1995). They may also influence water and protein solutions surface tension (Romero & Albis, 2010). These information suggested that sugar alcohols can affect the interfacial tension and phase equilibrium in ATP emulsions. Sugar alcohols are reduced form of sugars with an attached alcohol group in substitution to the aldehyde. Postprandially, they cause only a small change in blood sugar, which is especially beneficial for diabetics. However, ingestion of high amounts of these compounds can lead to bloating and diarrhea (Marcus, 2013). As an exception, erythritol is well (60–90%) and rapidly absorbed in the small intestine, which

makes it unlikely to observe the laxative side-effects associated with excessive consumption of other sugar alcohols. Erythritol is excreted intact into urine and does not enter blood circulation. Therefore, its glycemic index and caloric value are 0 and 0.2 kcal/g, respectively, against 100 and 3.9 kcal/g for sucrose. Erythritol is roughly 70% as sweet as sucrose with no after-taste (Grembecka, 2015). In addition to the conventional application as sweetener, sugar alcohols have been studied for their solubility in ionic liquids in biorefinery processes (Paduszyński, Okuniewski, Domańska, 2015), as phase-change materials for waste heat management (Nomura, Zhu, Sagara, Okinaka, & Akiyama, 2015) and as starch plasticizer and swelling inhibitory (Sun, Nan, Dai, Ji and Xiong, 2014).

The objective of the present study was to form ATP emulsions using a designed protein-rich aqueous phase, made incompatible with alginate droplets. This dispersant would be composed of hydrophobized whey protein (produced using a food-grade acetylating agent i.e. acetic anhydride), and erythritol, which is a low-calorie and naturally occurring zero-glycemic index sweetener. Interaction of protein particles with erythritol and the influence of erythritol on solvent properties were assessed by several techniques to understand how protein hydrophobization and erythritol addition synergistically favored ATP emulsion formation and stability.

2. Materials and methods

2.1. Materials

Whey protein isolate (WPI) powder was kindly gifted by Lactalis ingredients (Lactalis Group, Bourgbarré, France). It had 90% protein, 5.1% water, 3.0% lactose, and 1.97% ash contents in weight. Erythritol was purchased from Vita-World GmbH (Taunusstein, Germany). All chemicals used in the current study were analytical grade.

2.2. Protein acetylation

WPI solution (65 mg/mL) was hydrophobized by the procedure described elsewhere (Madadlou et al., 2018) with minor modifications and used for emulsification. Briefly, WPI solution (65 mg/mL) was titrated with acetic anhydride at an anhydride to protein ratio of ≈0.18 g/g. This was followed by gradual titration of the solution with 1 M NaOH to keep pH above 8.0 for 30 min. After the last titration, the WPI solution (pH ≈8.70) was heat-treated at 85°C for 20 min, which reduced pH to approximately 7.40. Heat-denatured (without acetylation) and native (not heated nor acetylated) WPI samples at pH 8.70 were also prepared and used in some experiments. The pH of the WPI samples was adjusted by either 1 M HCl (for native and heat-denatured samples) or NaOH (for hydrophobized sample) on to 8.30 ± 0.1 before emulsification.

2.3. Phase diagram

Different concentrations (0, 50, 100, 150, and 200 mg/g) of erythritol were added to the WPI solutions (native, heat-denatured and hydrophobized) and dissolved by vortexing. Then, the samples were supplemented with sodium alginate (1, 2, 3, 5, 7, 10, and 15 mg/g) and the mixtures were shaken overnight at 500 RPM and 20°C. Subsequently, the mixtures were centrifuged at 17,000 ×g for 30 min and the presence or absence of a fluid-fluid interface visible by the naked eye was noted. The phase diagram was plotted on dry basis using the triangular diagram of Extended UNIQUAC thermodynamic model (Thomsen & Rasmussen, 1999; Aqueous Solutions Aps, Søborg, Denmark) with Excel interface. The top and bottom phases were separately collected and read at 278 nm (UV−visible spectrophotometer, model UVmc2, SAFAS Monaco) to determine the protein- and alginate-rich phases.

2.4. Emulsification method

A series of preliminary tests were performed at different concentrations of WPI (35–65 mg/mL) and alginate (20–70 mg/mL), mixing speeds, mixing ratios of the two aqueous solutions, as well as various concentrations of NaCl (0, 50 and 100 mM) in the WPI solution

147 and several concentrations of erythritol. Accordingly, native, heated and hydrophobized (i.e.
148 acetylated + heated) WPI samples (65 mg/mL) were supplemented with different
149 concentrations (0, 52, 105 and 158 mg/g) of erythritol. Then, sodium alginate solution (30
150 mg/mL) was added as disperse phase (0.1 g) into WPI-erythritol mixed solution (0.9 g) and
151 the mixture was vortexed at 40 Hz (Bioblock Top Mix 11118, Fisher Scientific, Waltham,
152 MA, USA) for 2 min to obtain the ATP emulsion. Alternatively, the protein-polysaccharide
153 mixtures were homogenized at a high shear rate (30,000 rpm, IKA T 10 basic ULTRA-
154 TURRAX, IKA®-Werke GmbH & Co. KG, Staufen, Germany) but no difference was
155 observed between the droplet size of emulsions prepared by either vortex agitator or high-
156 speed homogenizer. Therefore, vortex agitation was used in the remainder of the study.

157 *2.5. Protein particle diameter and electric charge*

158 WPI samples with added erythritol were diluted 100 folds in distilled water and the
159 hydrodynamic diameter and ζ-potential of protein particles were measured by dynamic light
160 scattering (DLS) using a Zetasizer Nano ZS (Malvern Instruments Ltd., Worcestershire, UK).
161 A laser wavelength of 633 nm at backscattering angle of 173° was applied for size
162 measurements at 20°C and 38°C. The results are intensity-averaged values unless stated
163 otherwise.

164 *2.6. Intrinsic fluorescence spectroscopy*

165 The peak fluorescence emission wavelength (λ_{em}) and intensity of WPI solutions were
166 measured using a cuvette spectrofluorometer (FLX-Xenius, SAFAS Monaco, Monaco). WPI
167 samples were diluted 100 folds with distilled water, then supplemented with different
168 concentrations of erythritol, at erythritol to WPI ratios of 0:1, 3:1, 6:1, 11:1, 13:1, 21:1, 24:1,
169 30:1, and 34:1 and excited at 290 nm. Emission spectra were recorded at 300–400 nm with
170 the entrance and exit slits set at 10 nm. The fluorescence intensity of water as blank was
171 subtracted to correct background fluorescence.

172 *2.7. Viscosity measurement*

173 Viscosity of WPI samples was measured using a rotational viscometer with coaxial cylinders
174 system (LS 400 rheometer, Lamy Rheology, Champagne-au-Mont-d'Or, France) at 20°C.
175 Samples were sheared over the range of 2–100 s^{-1} and the obtained data were fitted to either
176 Newtonian (R≥0.999) or Power law (R≥0.999) models to determine their respective flow
177 behavior.

178 *2.8. Atomic force microscopy imaging*

179 Five µL of each suspension were spread over freshly cleaved mica (1×1 cm^2) then put in a
180 dessicator for at least 4 days. Imaging of the dessicated samples was performed using a
181 MFP3D-BIO AFM (Asylum Research, Santa Barbara, CA, USA) operated in AC mode and at
182 room temperature, using AC240TS silicon probes (Olympus, spring constant k ~2 $N.m^{-1}$, tip
183 radius ~9 nm). The typical scan rate was 0.5-1 Hz (2-20 µm/s) for 256 × 256 pixel images.
184 The images were typically plane-fitted at order 0 then flattened at order 1. Sections were
185 drawn across images to measure the apparent basal width and height of individual objects on
186 the images.

187 *2.9. Surface tension measurement*

188 Surface tension of WPI solutions was measured at 20°C by using a pendant drop tensiometer
189 ('Tracker' from Teclis- Scientific, France). Drops of 7 µL were formed at the tip of a syringe
190 containing the protein solutions. The drop profile was determined by image analysis, from
191 which the surface tension was derived. Under mechanical equilibrium of capillary and gravity
192 forces, the Laplace equation relates the pressure difference across the interface, the surface
193 tension and the surface curvature.

194 *2.10. Emulsion imaging*

195 Emulsion samples were imaged at room temperature (20°C) using a phase contrast optical
196 microscope equipped with an epifluorescence module (Olympus BX51TF, Olympus,

Hamburg, Germany) set at the magnification ×100. The imaging was carried out at non-fluorescent (bright field light microscopy) and fluorescent modes. For fluorescent imaging, an emulsion sample (90 μL) was stained with Fast Green FCF dye (1 w/v%, 10 μL) and imaged. The mean diameter of droplets was calculated by measuring the diameter of 20-40 droplets in each micrograph with Archimed software (version 7.1.1, Microvision Instruments, Evry cedex, France).

2.11. Statistical analysis

Samples were fabricated at least three times and the experiments were triplicated. The results were analyzed by One-way ANOVA with SPSS software version 16 (IBM software, NY, USA) using Duncan's test at a significance level of $p<0.05$.

3. Results on emulsion formation and stability

Native WPI and alginate formed homogenous protein-polysaccharide solutions at any concentration of erythritol (Fig. 1A), which reveals the compatibility of native whey proteins and alginate in our experimental conditions. Moreover, it has been demonstrated that native whey proteins cannot stabilize the interface of two immiscible aqueous solutions (Nguyen, Nicolai, & Benyahia, 2013). Considering that the expected interfacial tension should be extremely low between two immiscible aqueous solutions as opposed to oil-water interfaces (μN/m to be compared to mN/m) (Ganley et al., 2017) and that the particle size of native whey proteins is too small (Table 1), the adsorption energy of the protein on the interface remains low. Hence, native protein particles cannot stabilize ATP emulsions (Esquena, 2016). In agreement to our findings, mixing native WPI with co-charged polysaccharides (carrageenan or pectin) did not yield ATP emulsions (Chun et al., 2014).

Heat-treatment of whey proteins has been shown to promote phase separation and ATP formation (Thongkaew, Hinrichs, Gibis, & Weiss, 2015), which was attributed to the mitigation of depletion flocculation, as more space is available for polysaccharide chains

between two approaching thermally-induced protein filaments than between a pair of homogenous spheres of native whey proteins (Chun et al., 2014). However, alike native WPI, the mixed solution of heat-treated WPI and alginate at all erythritol concentrations was homogenous (Fig. 1A). In the current study, heat treatment did not produce long filamentous structures which are formed by heating at neutral pH (Chun et al., 2014), but yielded monodisperse spherical nano-particles (Table 1, section 4.1). In contrast to native and heat-denatured WPIs, hydrophobized (i.e. pre-acetylated and subsequently acetylated/heated) WPI solution was immiscible with alginate and formed ATP emulsion (Fig. 1B). However, the dispersed phase droplets coalesced rapidly and the emulsion phase separated into two distinct layers of protein and polysaccharide after 1 day. When the phase-separated samples were shaken by hand, remixing occurred, which indicates that the segregative phase separation was reversible. This reversibility has also been reported for a mixture of heat-denatured WPI and polysaccharides (Chun et al., 2014).

Figure 2 illustrates the ternary phase diagram of hydrophobized WPI, alginate and erythritol. The E-free and E-added WPI and alginate solutions were mixed, shaken and centrifuged. At alginate concentrations between 2 and 5 mg/g WPI solution, the mixtures separated into an upper phase rich in alginate and a lower phase rich in whey protein. However, at the alginate concentration of 7 mg/g WPI solution, a gel-like bottom phase was formed concomitant with the absence of the uppermost alginate phase. The supernatant (above the gel-like bottom phase) had a lower protein concentration than the protein-rich phase of the samples phase separated to two distinct liquid layers (data not reported). As well, the mass of the gel phase increased with increasing alginate concentration (7–15 mg/g WPI dispersion). These indicate that alginate structured to form the gel, entrapping protein. Formation of a bottom phase sediment by centrifugation is advantageous at separation and purification practices using the ATPS technique (Walker & Lyddiatt, 1998). A macroscopically monophasic solution was

obtained at the alginate concentration of 1 mg/g WPI dispersion. It is known that phase separation of protein and polysaccharide mixtures occurs only if the concentration of the biopolymers reaches relatively high values (Pacek, Ding, Nienow, & Wedd, 2000). The emulsion produced for microscopic imaging had an alginate content of 3 mg/g erythritol-free and erythritol-added hydrophobized WPI solution.

Erythritol addition into the hydrophobized WPI solution enhanced emulsion formation (Fig. 1 C & D). At the erythritol concentration of 52 mg/g, the droplet size was remarkably heterogeneous and in addition to many small droplets (≈1.0–3.0 μm), a few large drops (>10 μm) were observed in the microscopic images (Fig. 1C). Nonetheless, at the erythritol concentration of 105 mg/g, a highly stable emulsion (for at least 1 week) with less heterogeneous droplets (Fig. 1D) was produced. In Fig. 1C, the partial coalescence of two large drops in the 1st day of emulsion preparation is shown for the sample prepared at the erythritol concentration of 52 mg/g. Whereas, at 105 mg/g erythritol content, droplets evolved much slower, and the mean size of the droplets only reached 5 μm after 1 week storage at 20°C (Fig. 1F). The time evolution is consistent with the usual Ostwald ripening of dilute emulsions (with a size R scaling with time t such as $R \sim t^{1/3}$), which indicates that diffusion between the alginate droplets contributed to the droplet size growth.

We identified by fluorescent microscopy imaging (Fig. 1G) that whey proteins formed the continuous phase, while phase inversion and mixing of the aqueous phases did not occur over storage of the emulsion. In contrast to the opaque and milky appearance of oil-water emulsions, the ATP emulsions because of small difference in the refractive index of the two aqueous phases (Singh et al., 2018) were rather transparent. A bi-continuous ATP emulsion was obtained at the highest concentration (i.e. 158 mg/g) of erythritol (Fig. 1E).

4. Complementary results: protein particles, bulk and interfacial properties

At this stage, a variety of experiments were carried out to explain why WPI hydrophobization caused ATP emulsion formation, and how the addition of erythritol to the hydrophobized WPI solution helped to form the emulsion. However, one should keep in mind that erythritol would partition between the WPI-rich and alginate-rich phases. Protein and alginate also partition between the phases, which will result in complex multi-component phases. Therefore, the information provided here mainly address the emulsification stage and further investigations must be performed to describe the behavior of the emulsion over storage.

4.1. Protein particle characteristics and viscosity

The number-averaged particle diameter of the control native WPI was found to be approximately 2.9 nm. Heating and hydrophobization (i.e. pre-acetylation and subsequent acetylation/heating) processes resulted in formation of whey protein nano-particles of approximately 57 and 80 nm Z-average diameter (which is the intensity-weighted arithmetic average diameter of particles), respectively (Table 1). In DLS, the intensity decay rate Γ of the scattered light is used to obtain the diffusion coefficient D of freely floating particles in a suspension:

$$\Gamma = q^2 D \qquad \text{[Eq. 1]}$$

where q is the modulus of scattering vector. When qR becomes substantially larger than 1, relaxation of particles internal structure contributes to Γ. In the current study, qR had a maximum value of 1.2, indicating that the intensity relaxation derived mainly from the particles Brownian motion. However, it is noteworthy that the z-average radius is underestimated at values smaller than q^{-1}., which was 38 nm in this study. There was no difference between the polydispersity indices of heat-denatured and hydrophobized particles. Results on particle size, surface hydrophobicity and electric charge, free amino groups content, and structural characteristics of the protein particles have been comprehensively discussed elsewhere (Madadlou et al., 2018). Protein nano-particles made by either heating or

the hydrophobization process were slightly smaller at 38°C than 20°C (Table 1; $p<0.05$). Likewise, intrinsic viscosity and voluminosity data have suggested a slight shrinkage of thermally treated whey proteins upon temperature increase (Eissa, 2013). The DLS method calculates the hydrodynamic diameter of particles and takes account of the hydration layer (Fissan, Ristig, Kaminski, Asbach, & Epple, 2014). Enhancement of the strength of the constitutive hydrophobic interactions and/or partial dehydration of the protein particles could decrease their Z-average diameter at the higher temperature. On the contrary, the mean particle size of native whey proteins increased at 38°C in comparison to the ambient condition. Increasing temperature to 38°C approximately doubled the particle size of native whey proteins (Table 1; $p <0.05$). We propose that hydrophobic interactions among the partially unfolded protein monomers (in the alkaline conditions) were enhanced at the higher temperature, resulting in dimer and multimer formation.

Sugar alcohols may interact with amino acids through hydrophilic-ionic (between *–OH* groups of sugar alcohol and NH_3^+ and COO^- groups of amino acids), hydrophobic-hydrophobic (between *CH* groups of sugar alcohols and non-polar side chains of amino acids) and hydrophilic-hydrophobic interactions (Ali & Bidhuri, 2013). Nonetheless, erythritol addition did not influence the Z-average diameter, polydispersity index and ζ-potential of whey protein nano-particles at either 20°C or 38°C (Table 1), which suggests that erythritol did not interact electrostatically with WPI particles. As well, the intrinsic fluorescence emission peak (λ_{em}) and intensity of WPI samples were not influenced by erythritol addition at different ratios of erythritol to WPI (Table 2). The shift of λ_{em} from 329 nm to 334 nm due to heat treatment has been ascribed to whey protein denaturation and increased exposure of Trp residues. Also, the bathochromic shift of λ_{max} due to hydrophobization was ascribed to a less compact tertiary conformation of acetylated protein (Madadlou et al., 2018). Fluorescence spectroscopy is a sensitive and rapid method to study molecular interactions

involving proteins. Measurement of intrinsic fluorescence quenching of a protein by ligands allows assessment of the accessibility of quenchers to fluorophore groups of the protein, mediated largely by hydrophobic forces (Zhang, Que, Pan, & Guo, 2008). Hydrophobic interaction between a ligand and a protein decreases fluorescence intensity and may cause a blue shift in the emission wavelength (Cui, Fan, Li, & Hu, 2004). The unchanged λ_{em} and intensity (Table 2) indicates that erythritol did not interact hydrophobically with WPI particles. In addition to concluding no interaction between erythritol and WPI particles, one may assume (based on the DLS and intrinsic fluorescence results) that erythritol addition did not influence interaction amongst the protein particles. Nonetheless, it is worth mentioning that samples were diluted before DLS measurements; thus, the results do not reflect the possible effect of erythritol on supramolecular organization of protein particles at a high WPI concentration. Therefore, viscosity measurement was also used to probe the organization of protein particles in non-diluted conditions.

As tabulated (Table 1), the viscosities of all WPI (native, heat-treated and hydrophobized) samples without added erythritol were independent from shear rate, indicating that the samples were Newtonian fluids. Identical rheological behavior has been reported for whey protein concentrate (WPC) solutions (Benoit, Nor Afizah, Ruttarattanamongkol, & Rizvi, 2013). Heat treatment and hydrophobization increased the viscosity of WPI solution, due to formation of larger nano-particles compared to native whey proteins (Table 1).

The flow property of WPI solutions was affected by erythritol addition (Table 1). Erythritol addition (at 105 mg/g) caused an approximately 1.3-fold increase of the viscosity of native and heat-treated WPI solutions but the samples kept a Newtonian behavior. Similarly, the hydrophobized WPI solution with the lowest concentration of added erythritol (52 mg/g) had Newtonian flow behavior and exhibited a higher viscosity than the counterpart without erythritol. In contrast, addition of erythritol to hydrophobized WPI solution at concentrations

of ≥105 mg/g, changed the solution to a non-Newtonian fluid (Table 1). Although the viscosity of hydrophobized WPI with 105 mg/g erythritol decreased with increasing shear rate (Fig. 3), it always (at any shear rate) had a significantly higher viscosity than the native and heat-treated samples with a comparable concentration of added erythritol. The shear thinning property of the hydrophobized WPI solutions with ≥105 mg/g erythritol was weak (Won & Kim, 2004). Non-ionic low-molecular weight osmolytes such as erythritol alter solvent features and may cause steric crowding of biomacromolecules such as proteins due to osmolytes exclusion from the protein surface (Ferreira, Breydo, Reichardt, Uversky & Zaslavsky, 2016). It is also known that high concentrations of solutes because of excluding water modulate protein-protein binding (Hassan & Steinbach, 2011). We hypothesize that erythritol addition at a sufficiently high concentration (i.e. ≥105 mg/g) into WPI solution caused macromolecular crowding of proteins, inducing interaction between hydrophobized WPI nano-particles through their acetyl moieties. Direct interaction of solute (i.e. erythritol) with proteins was not necessary to enhance the hydrophobic effect (Eggers & Valentine, 2001). The interactions between protein particles impaired the movement of water solvent at low shear rates. Likewise, reduction of the micellization concentration of amphiphiles by sugars has been ascribed to the enhancement of hydrophobic interactions (Kabir-ud-Din, Khan, & Navqi, 2012).

4.2. AFM imaging

Although erythritol did not directly interact with WPI particles, it was hypothesized (from the viscosity measurement results) that at the erythritol concentration of 105 mg/g, interactions between hydrophobized protein particles were enhanced. AFM was applied to visualize protein particles and acquire information about the influence of erythritol on the morphology and association of WPI particles. Where erythritol (E) and native WPI (N) was deposited on mica, the rugosity indicates some material on the mica; therefore, both erythritol and WPI

were adsorbed (Fig. 4, comparing E or N with mica) and no further step was required for the successful immobilization of the objects.

Air-dried erythritol formed thick crystal-like structures of irregular shape and rugosity of tens of nm order of magnitude (Fig. 4E). Similar irregular surfaces containing areas with pits and asperities have been observed by tapping mode AFM imaging of lactose monohydrate and erythritol (Traini, Young, Jones, Edge, & Price, 2006). Native WPI deposits showed rather low rugosities (~2 nm; Fig. 4N) in agreement with other reports (Ikeda & Morris, 2002; Demanèche, Chapel, Monrozier, Quiquampoix, 2009; Touhami & Dutscher 2008). Rugosity of the WPI layer increased with heat denaturation and hydrophobization (acetylation/heating) to reach 4-5 nm (Fig. 4H and A/H). In the AFM images, the dimensions of heat-denatured and hydrophobized WPIs without erythritol (Fig. 4H and A/H) were much smaller than their corresponding Z-average diameter (Table 1). Likewise, considerably shorter heights (only 11 nm) were estimated using AFM images for whey protein aggregates formed by heating than what was expected from the results of light scattering studies (Ikeda, 2003). Ikeda & Morris (2002) argued that vertical compression of proteins by the scanning probe of the microscope accounts for the height reduction (approximately 40%) of native β-lactoglobulin particles. In addition to the probe compression, particle deformation upon adsorption onto the mica can decrease the height and increase the width of protein particles, especially that there was no covalent binding (Silva, Bahri, Guyomarc'h, Beaucher, & Gaucheron, 2015). Finally, dehydration of samples before AFM imaging probably shrunk the WPI particles. It is worth mentioning that particles of hydrophobized WPI were more distinguishable at AFM images than heat-denatured and native WPI particles (Fig. 4N, H and A/H). This suggests that hydrophobized particles could retain their shape despite compression and flattening, and were comparatively firmer than the other two samples.

A greater rugosity is observed for each sample in the presence of erythritol compared to erythritol-free conditions (Fig. 4, compare N with N+E, H with H+E and A/H with A/H+E). We argue that some erythritol scaffolds the WPI particles, helping them to retain their shape upon drying. This hypothesis resembles the vitrification mechanism according which, an amorphous glassy matrix is formed by sugars around proteins during drying, resulting in preservation of the protein structure (Mensink, Frijlink, Maarschalk, & Hinrichs, 2017). Using the visible height and width of individual particles seen on the images, the volume of the corresponding spherical cap was calculated, from which the diameter of a sphere of equivalent volume was deduced (Silva et al., 2015). A diameter value of 10–20 nm was obtained for erythritol-added native (N+E) and heat-denatured (H+E) samples, against 150 nm for A/H+E (i.e. erythritol-added hydrophobized WPI). The latter is larger than the corresponding Z-average diameter of the hydrophobized particles (Table 1) and may indicate aggregates of particles, supporting our presumption that particles interacted by their acetyl moieties.

4.3. Surface tension of WPI solutions

Data from the surface tension measurements are represented in Figure 5. Pure water (containing NaN_3 at 100 mg/L to match the composition of WPI samples) had a surface tension of approximately 73.1 mN/m. All WPI samples showed an initial rapid reduction in surface tension, followed by a gradual decrease over time. It might require time periods as long as 120 min to reach a constant surface tension value by protein solutions. Proteins diffuse to the surface of freshly formed droplets, and then undergo conformational changes and structural rearrangements (Kitabatake & Doi, 1982) to increase the number of contact points at the air/water interface (Schröder, Berton-Carabin, Venema, & Cornacchia, 2017) during surface aging, which reduces surface tension. The results (Fig. 5) obtained for native and heat-denatured WPI samples are typical for proteins (Nylander, Hamraoui, & Paulsson,

1999). Heat-denaturation and hydrophobization decreased the surface tension of WPI solution. The liquid-air interface is indeed a very hydrophobic surface (Chanasattru, Decker, & McClements, 2008); hence, a lower surface tension value indicates a higher degree of protein hydrophobicity. A correlation between surface activity and surface hydrophobicity has already been observed for whey proteins (Schröder et al., 2017) and as expected, hydrophobization (i.e. pre-acetylation and subsequent acetylation/heating combined process) that caused a more significant increase in surface hydrophobicity of whey proteins than only heating (Madadlou et al., 2018a) resulted in a greater reduction of surface tension. The surface tension of hydrophobized WPI sample was approximately 48 mN/m after ageing of droplet for 350 seconds. The results suggest that hydrophobized protein particles could adsorb to the WPI-alginate interface, forming a layer that decreased the alginate droplets coalescence.

Erythritol addition to water (105 mg/g) caused a slight reduction of surface tension from about 73 mN/m to 71.5 (Fig. 5), meaning that erythritol has a low surface activity. Similarly, Yamada, Fukusako, Kawanami, Sawada, and Horibe (1997) observed that D-sorbitol (100 mg/g) decreased the surface tension of water from ≈73 mN/m to 70.1 mN/m at 20°C. Evacuation of a number of erythritol molecules to the air-water interface due to the imperfect fitting of the solute molecules within the tetrahedral structure of water (Brini et al., 2017) explains the observed result.

Erythritol addition decreased the surface tension of native and heat-treated samples to approximately that of hydrophobized WPI solution without added erythritol. As well, for the hydrophobized WPI sample, we found that the higher the erythritol content, the lower the surface tension (Fig. 5), so that, the surface tension values of hydrophobized WPIs with 105 and 158 mg/g erythritol were about 45 and 43.5 mN/m, respectively after ageing of droplet for 350 seconds. Therefore, the surface tension of the hydrophobized WPI solution decreased by a value of 3 mN/m as a consequence of adding erythritol at 105 mg/g concentration, which is

445 an effect twice larger that what erythritol does on its own at the interface. Thus, the decrease
446 of surface tension, when erythritol is added, cannot be ascribed to a simple co-adsorption of
447 erythritol at the interface, together with whey proteins. As for viscosity, erythritol modify the
448 interaction between particles, providing structures more hydrophobic. When a cosolvent is
449 added to an aqueous protein solution, chemical potentials of the cosolvent and protein are
450 mutually perturbed. Osmolytes such as sugars and polyols show a greater affinity to water;
451 thus, they are preferentially excluded from protein surface. This causes a negative
452 perturbation of the chemical potential of protein (Timasheff, 2002) which increases free
453 energy and renders system thermodynamically more unfavorable. As the driving force of
454 protein adsorption to interface is the chemical potential gradient between the bulk and
455 interface, an increase in the chemical potential of the proteins in solution increases the
456 adsorption gradient, which can led to an increased adsorbed amount of the protein onto air-
457 water interface (Abbas, Sharma, Patapoff, & Kalonia, 2012).

458 The dynamic surface tension of the WPI solution with added erythritol at the concentration of
459 158 mg/g was lower than that of the WPI sample with 105 mg/g erythritol during the whole
460 period of droplet aging. Nonetheless, the former failed to form an alginate-in-WPI emulsion
461 with discrete dispersed droplets (Fig. 1). Therefore, lower and lower surface tensions are not
462 the only requirements to make long-living emulsion. We argue that a balance between
463 viscosity and surface tension was essential to produce an ATP emulsion. The significantly
464 high viscosity of the WPI sample containing 158 mg/g erythritol prevented the Rayleigh-
465 Plateau instability, which usually leads to discrete droplets. Indeed, surface tension has to be
466 balanced by the viscous effects, which act during the emulsification.

467 We made an effort to measure the interfacial tension between the alginate and hydrophobized
468 WPI phases. However, the experiment failed because the alginate solution injected into the
469 hydrophobized WPI could not provide a typical shape, resulting from the balance between

surface tension and gravity (Fig. 6). The shape of rising or pending drops moving is characterized by the Bond number, which measures the balance between these interfacial and gravitational forces:

$$Bo = \frac{\Delta\rho g L^2}{\gamma} \quad \text{[Eq. 2]}$$

where $\Delta\rho$, g, L^2 and γ are density difference between the disperse and surrounding phases (kg/m^3), gravitational acceleration (m/s^2), characteristic length (m), and interfacial tension (N/m), respectively.

The needle of the pendant drop tensiometer used in the current study had a section of 1 mm. Hence, the drops had a typical length scale L of 1 mm. At this scale, gravity turns out to be too strong to be balanced by surface tension, meaning that the interfacial tension of the two aqueous phases has to be in the range of μN/m, rather than the usual mN/m for oil-water emulsions. As a consequence, no stable drops could be made and the lighter fluid (i.e. alginate) simply raised upward. Nonetheless, the apparatus allowed us to observe that the two fluids were not spontaneously miscible; one can identify an interface between them (Fig. 6). The observed time evolution (Fig. 1F) consistent with the classical Ostwald ripening, is also an indirect signature of the existence of the interfacial tension between WPI and alginate (in the presence of erythritol). During emulsion formation, as the typical length scale of the generated drops was μm, the influence of interfacial tension was recovered. Indeed, the relevant quantity to estimate is γ/L, rather than only γ itself.

The interfacial stresses can also be compared to viscous ones by the Capillary number:

$$Ca = \frac{\mu V}{\gamma} \quad \text{[Eq. 3]}$$

where μ and V are the fluid dynamic viscosity and velocity, respectively. It is observed in Fig. 1E that when the interfacial stresses are too low compared to the viscous component, the

impact of having an interfacial tension vanishes and spherical drops (which are the signature that surface tension plays a role) could not be created. Instead, in a viscous-dominated regime, the elongated ligaments were formed. Lastly, we want to point out that the measurements of the surface tension between WPI and air was still helpful, as it gave us important information on how the hydrophobicity depended on the experimental conditions (presence of erythritol, concentration, etc.).

4. Summary and conclusion

Hydrophobization of whey proteins was found effective to cause immiscibility of WPI solution with alginate solution, but the resulting W/W emulsion was destabilized within 24 h. Addition of erythritol strongly helped the emulsification and increased the stability of the resulting emulsion. At the first glance, erythritol does not interact with WPI particles. However, some further works are needed to fully understand the influence of erythritol on WPI particles. It was concluded that erythritol addition into WPI solution enhanced emulsification by a further increase of the hydrophobicity of the WPI particles, promoting phase separation and the occurrence of a non-zero (but extremely low) surface tension between the two phases. It also improved the emulsion stability by reducing droplets coalescence due mainly to increased viscosity. Nonetheless, a balance between viscosity of the continuous phase (WPI solution) and the interfacial tension was essential to accomplish efficient emulsification because higher viscosities of the WPI phase prevented the miniaturization of alginate phase. The developed ATP emulsion can serve as a delivery vehicle of bioactive compounds and other ingredients to diabetics, obese and elderly people because it does not contain oil and absorbable sweetener.

Acknowledgements

The authors are thankful to the support of the EU in the framework of the Marie-Curie FP7 COFUND People Programme, through the award of an AgreenSkills+ fellowship (grant agreement n°609398).

The Asylum Research MFP3D-BIO atomic force microscope was funded by the European Union (FEDER), the French Ministry of Education and Research, INRA, Conseil Général 35 and Rennes Métropole.

References

Abbas, S.A., Sharma, V.K., Patapoff, T.W., & Kalonia, D.S. (2012). Opposite effects of polyols on antibody aggregation: Thermal versus mechanical stresses. *Pharmaceutical Research*, 29, 683–694.

Ali, A. & Bidhuri, P. (2013). Solvation thermodynamics of xylitol in water and in aqueous amino acids at 298.15 K. *Journal of Physical Organic Chemistry*, 26, 54-58.

Benoit, S. M., Nor Afizah, M., Ruttarattanamongkol, K., & Rizvi, S. S. H. (2013). Effect of pH and temperature on the viscosity of texturized and commercial whey protein dispersions. *International Journal of Food Properties*, 16, 322-330.

Brini, Fennell, Fernandez-Serra, Hribar-Lee, Lukšič, & Dill, K. A. (2017). How water's properties are encoded in its molecular structure and energies. *Chemical Reviews*, 117, 12385–12414.

Chanasattru, W., Decker, E.A., & McClements, D.J. (2008). Impact of cosolvents (polyols) on globular protein functionality: Ultrasonic velocity, density, surface tension and solubility study. *Food Hydrocolloids*, 22, 1475–1484.

Chun, J.-Y., Hong, G.-P., Surassmo, S., Weiss, J., Min S.-G., & Choi, M.-J. (2014). Study of the phase separation behaviour of native or preheated WPI with polysaccharides. *Polymers*, 55, 4379–4384.

Cioci, F. (1995). Catalytic activity of *Aspergillus niger* glucose oxidase in water-polyol mixtures. *Catalysis Letters*, 35, 395–405.

Cui, F.-L., Fan, J., Li, J.-P., Hu, Z.-D. (2004). Interactions between 1-benzoyl-4-*p*-chlorophenyl thiosemicarbazide and serum albumin: investigation by fluorescence spectroscopy. *Bioorganic and Medicinal Chemistry*, 12, 151–157.

de Freitas, R.A., Nicolai, T., Chassenieux, C., & Benyahia, L. (2016). Stabilization of water-in-water emulsions by polysaccharide-coated protein particles. *Langmuir*, 32, 1227–1232.

Demanèche, S., Chapel, J.-P., Monrozier, L. J., & Quiquampoix, H. (2009). Dissimilar pH-dependent adsorption features of bovine serum albumin and α-chymotrypsin on mica probed by AFM. *Colloids & Surface B: Biointerfaces*, 70, 226–231.

Dewey, D. C., Strulson, C. A., Cacace, D. N., Bevilacqua, P. C., & Keating, C. D. (2014). Bioreactor droplets from liposome-stabilized all-aqueous emulsions. *Nature Communications*, 5, 4670.

Eggers, D. K., & Valentine, J. S. (2001). Crowding and hydration effects on protein conformation: a study with sol-gel encapsulated proteins. *Journal of Molecular Biology*, 314, 911–922.

Eissa, A.S. (2013). Newtonian viscosity behavior of dilute solutions of polymerized whey proteins. Would viscosity measurements reveal more detailed molecular properties? *Food Hydrocolloids*, 30, 200–205.

Esquena, J. (2016). Water-in-water (W/W) emulsions. *Current Opinion in Colloid & Interface Science*, 25, 109–119.

Ferreira, L. A., Breydo, L., Reichardt, C., Uversky, V. N., & Zaslavsky, B. Y. (2016). Effects of osmolytes on solvent features of water in aqueous solutions, *Journal of Biomolecular Structure and Dynamics*, 35, 1055-1068.

Firoozmand, H., Murray, B.S., and Dickinson, E. (2009). Interfacial structuring in a phase separating mixed biopolymer solution containing colloidal particles. *Langmuir*, 25, 1300–1305.

Fissan, H., Ristig, S., Kaminski, H., Asbach, C., & Epple, M. (2014). Comparison of different characterization methods for nanoparticle dispersions before and after aerosolization. *Analytical Methods*, 6, 7324-7334.

Ganley, W.J., Ryan, P.T., & van Duijneveldt, J.S. (2017). Stabilisation of water-in-water emulsions by montmorillonite platelets. *Journal of Colloid & Interface Science*, 505, 139–147.

Gekko, K. (1981). Mechanism of polyol-induced protein stabilization: Solubility of amino acids and diglycine in aqueous polyol solutions. *Journal of Biochemistry*, 90, 1633–1641.

Grembecka, M. (2015). Sugar alcohols—their role in the modern world of sweeteners: a review. *European Food Research and Technology*, 241, 1–14.

Grinberg, V.Ya., and Tolstoguzov, V.B. (1997). Thermodynamic incompatibility of proteins and polysaccharides in solutions. *Food Hydrocolloids*, 11, 145–158.

Hassan, S. A., & Steinbach, P. J. (2011). Water-exclusion and liquid-structure forces in implicit solvation. *Journal of Physical Chemistry B*, 115, 14668–14682.

Ikeda, S. (2003). Heat-induced gelation of whey proteins observed by rheology, atomic force microscopy, and Raman scattering spectroscopy. *Food Hydrocolloids*, 17, 399–406.

Ikeda, S. & Morris, V. J. (2002). Fine-stranded and particulate aggregates of heat-denatured whey proteins visualized by atomic force microscopy. *Biomacromolecules*, 3, 382–389.

Kabir-ud-Din; Khan, A.B., & Navqi, A.Z. (2012). Solution and surface properties of amphiphilic drug – nonelectrolyte systems. *Physics and Chemistry of Liquids*, 50, 478–494.

Kitabatake, N & Doi, E. (1982). Surface tension and foaming of protein solutions. *Journal of Food Science*, 47, 1218-1221.

Madadlou, A., Floury, J., and Dupont, D. (2018). Structural assessment and oxidation catalytic activity of hydrophobized whey proteins. *Journal of Agricultural & Food Chemistry*. 66 (45), 12025–12033, DOI: 10.1021/acs.jafc.8b02362

Marcus, J.B. (2013). *Carbohydrate Basics: Sugars, Starches and Fibers in Foods and Health Healthy Carbohydrate Choices, Roles and Applications in Nutrition, Food Science and the Culinary Arts*, IN Culinary Nutrition. Pages 149–187. Elsevier, Tokyo.

Mensink, M. A., Frijlink, H. W., Maarschalk, K. v., & Hinrichs, W. L. J. (2017). How sugars protect proteins in the solid state and during drying (review): Mechanisms of stabilization in relation to stress conditions. *European Journal of Pharmaceutics & Biopharmaceutics*, 114, 288–295.

Moschakis, T., Chantzos, N., Biliaderis, C.G., and Dickinson, E. (2018). Microrheology and microstructure of water-in-water emulsions containing sodium caseinate and locust bean gum. *Food & Function*, 9, 2840–2852.

Mytnyk, S., Olive, A.G.L., Versluis, F., Poolman, J.M., Mendes, E.,Eelkema, R., and van Esch J.H. (2017). Compartmentalizing supramolecular hydrogels using aqueous multiphase systems. *Angewandte Chemie International Edition*, 56, 14923–14927.

Nomura, T., Zhu, C., Sagara, A., Okinaka, N., & Akiyama, T. (2015). Estimation of thermal endurance of multicomponent sugar alcohols as phase change materials. *Applied Thermal Engineering*, 75, 481–486.

Nguyen, B.T., Nicolai, T., & Benyahia, L. (2013). Stabilization of water-in-water emulsions by addition of protein particles. *Langmuir*, 29, 10658–10664.

Nicolai, T. and Murray, B. (2017) Particle stabilized water in water emulsions. *Food Hydrocolloids*, 68, 157–163.

Nylander, T., Hamraoui, A. and Paulsson, M. (1999). Interfacial properties of whey proteins at air/water and oil/water interfaces studied by dynamic drop tensiometry, ellipsometry and spreading kinetics. *International Journal of Food Science & Technology*, 34, 573-585.

Pacek, A. W., Ding, P., Nienow, A. W. and Wedd, M. (2000). Phase separation and drop size distributions in "homogeneous" Na-alginate/Na-caseinate mixtures. *Carbohydrate Polymers*, 42, 401–409.

Paduszyński, K., Okuniewski, M., & Domańska, U. (2015). Solid–liquid phase equilibria in binary mixtures of functionalized ionic liquids with sugar alcohols: New experimental data and modelling. *Fluid Phase Equilibria*, 403, 167–175.

Poortinga, A.T. (2008). Microcapsules from self-assembled colloidal particles using aqueous phase-separated polymer solutions. *Langmuir*, 24, 1644–1647.

Romero, C.M. and Albis, A. (2010). Influence of polyols and glucose on the surface tension of bovine *α*-lactalbumin in aqueous solution. *Journal of Solution Chemistry*, 39, 1865-1876.

Schröder, A., Berton-Carabin, C., Venema, P., & Cornacchia, L. (2017). Interfacial properties of whey protein and whey protein hydrolysates and their influence on O/W emulsion stability. *Food Hydrocolloids*, 73, 129-140.

Silva, N. N., Bahri, A., Guyomarc'h, F., Beaucher, E., & Gaucheron, F. (2015). AFM study of casein micelles cross-linked by genipin: effects of acid pH and citrate. *Dairy Science & Technology*, 95, 75-86.

Singh, P., Medronho, B., Miguel, M.G., and Esquena, J. (2018). On the encapsulation and viability of probiotic bacteria in edible carboxymethyl cellulose-gelatin water-in-water emulsions. *Food Hydrocolloids*, 75, 41–50.

Song, Y., Shimanovich, U., Michaels, T. C. T., Ma, Q., Li, J.,Knowles, T. P. J., & Shum, H. C. (2016). Fabrication of fibrillosomes from droplets stabilized by protein nanofibrils at all-aqueous interfaces. *Nature Communications*, 7, 12934.

Spicer, C.D. and Davis, B.G. (2014). Selective chemical protein modification. *Nature Communications*, 5, 4740.

Sun, Q., Nan, C., Dai, L., Ji, N., and Xiong, L. (2014). Effect of sugar alcohol on physicochemical properties of wheat starch. *Starch/Stärke*, 66, 788–794.

Thomsen, K. & Rasmussen, P. (1999). Modeling of vapor–liquid–solid equilibrium in gas–aqueous electrolyte systems. *Chemical Engineering Science*, 54, 1787–1802.

Thongkaew, C., Hinrichs, J., Gibis, M., & Weiss, J. (2014). Sequential modulation of pH and ionic strength in phase separated whey protein isolate – Pectin dispersions: Effect on structural organization. *Food Hydrocolloids*, 47, 21–31.

Touhami, A. & Dutcher, J. R. (2009). pH-induced changes in adsorbed β-lactoglobulin molecules measured using atomic force microscopy. *Soft Matter*, 5, 220–227.

Traini, D., Young, P.M., Jones, M., Edge, S., & Price, R. (2006). Comparative study of erythritol and lactose monohydrate as carriers for inhalation: Atomic force microscopy and in vitro correlation. *European Journal of Pharmaceutical Sciences*, 27, 243–251.

658 Tyagi, R., & Gupta M. N. (1998). Chemical modification and chemical cross-linking for
659 protein/enzyme stabilization. *Biochemistry-Moscow*, 63, 334–344.

660 Walker, S. G., & Lyddiatt, A. (1998). Aqueous two-phase systems as an alternative process
661 route for the fractionation of small inclusion bodies. *Journal of Chromatography B:*
662 *Biomedical Sciences and Applications*, 711, 185–194.

663 Walstra, P. (2003). *Physical chemistry of foods.* New York: Marcel Dekker, (Chapter 6).

664 Won, D., & Kim, C. (2004). Alignment and aggregation of spherical particles in viscoelastic
665 fluid under shear flow. *Journal of Non-Newtonian Fluid Mechanics*, 117, 141-146.

666 Yamada, M., Fukusako, S., Kawanami, T., Sawada, I., & Horibe, A. (1997). Surface tension
667 of aqueous binary solutions. *International Journal of Thermophysics*, 18, 1483–1493.

668 Zhang, G., Que, Q., Pan, J., & Guo, J. (2008). Study of the interaction between icariin and
669 human serum albumin by fluorescence spectroscopy. *Journal of Molecular Structure*, 881,
670 132–138.

671

672

Table 1. Particle size and ζ-potential of protein particles and the viscosity (at 20°C and between 2-100 s^{-1}) of whey protein isolate (WPI) samples.

WPI sample[1] + erythritol (mg/g) content	Particle size; PDI		ζ-potential (mV)	Flow behavior	Viscosity (mPas)
	20°C	38°C			
N + 0	2.9 ± 0.3	6.4 ± 1.4	-26.1^{c} ± 2.6	Newtonian	1.47^{h} ± 0.1
N + 105	2.9 ± 0.2	6.1 ± 1.8	-25.9^{c} ± 2.9	Newtonian	1.92^{g} ± 0.1
H + 0	62.1^{cd} ± 1.2; 0.24	60.1^{de} ± 1.41; 0.23	-34.8^{b} ± 1.1	Newtonian	2.07^{f} ± 0.1
H + 105	62.7^{c} ± 1.6; 0.24	58.5^{e} ± 1.77; 0.21	-33.9^{b} ± 2.0	Newtonian	2.72^{e} ± 0.1
A/H + 0	87.2^{a} ± 3.1; 0.23	82.6^{b} ± 2.6; 0.22	-40.2^{a} ± 1.9	Newtonian	4.90^{b} ± 0.15
A/H + 52	88.4^{a} ± 2.0; 0.22	82.6^{b} ± 1.7; 0.23	-40.4^{a} ± 2.4	Newtonian	5.23^{a} ± 0.1
A/H+ 105	88.9^{a} ± 1.5; 0.23	82.9^{b} ± 2.0; 0.22	-40.8^{a} ± 1.6	Shear-thinning	See Fig. 3
A/H + 158	89.6^{a} ± 1.5; 0.23	83.1^{b} ± 0.8; 0.23	-40.2^{a} ± 1.2	Shear-thinning	See Fig. 3

[1] N = Native; H = Heated; A/H = Acetylated/heated (hydrophobized) WPI samples.
Means with different superscripts within a column differ significantly ($p < 0.05$).

Table 2. Intrinsic fluorescence emission peak (λ_{em}) and intensity of whey protein isolate (WPI) samples mixed with erythritol (E) at different ratios of E to WPI between 0:1 and 34:1.

WPI sample[1] + erythritol (w/w%) content	**λ_{em} (nm)**	**Emission intensity (A.U.)**
N + 0	329 ± 0	44.1 ±1.2
N + E	329 ± 0	44.3 ±1.6
H + 0	334 ± 0	13.7 ± 0.3
H + E	334 ± 0	14.4 ± 1.0
A/H + 0	335 ± 0	25.5 ±0.9
A/H + E	335 ± 0	23.6 ±0.8

[1] N = Native; H = Heated; A/H = Acetylated/heated (hydrophobized) WPI samples.

Figure captions

Fig. 1. Light microscopy images of alginate (30 mg/mL) and whey protein isolate (WPI) mixed solutions with added erythritol. All samples contained alginate solution at 10 w/w %.

The image A is an exemplar image showing homogenous solutions of alginate and either native or heat-denatured WPI supplemented with erythritol (0–158 mg/g).

The images B, C, D and E show emulsions of alginate-in-hydrophobized (acetylated and heat-treated) WPI containing 0, 52, 105 and 158 mg/g erythritol, respectively.

The image F plots droplet size of the alginate-in-hydrophobized WPI emulsion with 105 mg/g added erythritol over storage for 1 week and the solid line is a power law fit (t^a), and the fitting exponent is a = 0.35.
The image G shows exemplar epi-fluorescent microscopy images of the emulsion containing 105 mg/g erythritol at day 7.

Fig. 2. Phase diagram of hydrophobized protein (acetylated and heat-treated whey protein isolate), sodium alginate and erythritol after centrifugation. The hatched area confining the circles identifies combinations of the components that yielded immiscible liquid-liquid phases. The cubes indicate the combinations that yielded a gel-like bottom phase and a liquid supernatant phase, and the triangle indicates the combination that yielded a mono-phasic solution. The phase diagram was plotted on dry basis.

Fig. 3. Viscosity vs. shear rate ($\dot{\gamma}$) of hydrophobized whey protein isolate (A/H WPI) solutions supplemented with erythritol at 105 mg/g and 158 mg/g WPI solution. The measurement were carried out at 20°C; lines are power law fits, providing the values of *n* and K (respectively, the flow index and the consistency coefficient of the samples).

Fig. 4. Atomic force microscopy images. Aspect of dessicated deposits of native (N), heated (H) and acetylated/heated (A/H) whey protein samples (65 g/L) spread onto mica (shown as control image), in absence (left) and presence (right) of 105 mg/g erythritol (E). Typical 2D and 3D topographical images as well as a typical 1-µm cross-section are shown for each type of sample. Mind the scales which can differ, especially for E and A/H+E.

Fig. 5. Surface tension of whey prtoein isolate (WPI) solutions as a function of time. N, H and A/H abbreviate native, heat-denatured and hydrophobized (acetylated/heated) WPI samples, respectively and the values report the concentration of erythritol (mg/g) addedd into WPI samples.

Fi. 6. The image of an alginate drop injected by a needle of the pendant drop tensiometer into the hydrophobized whey protein isolate (WPI) phase.

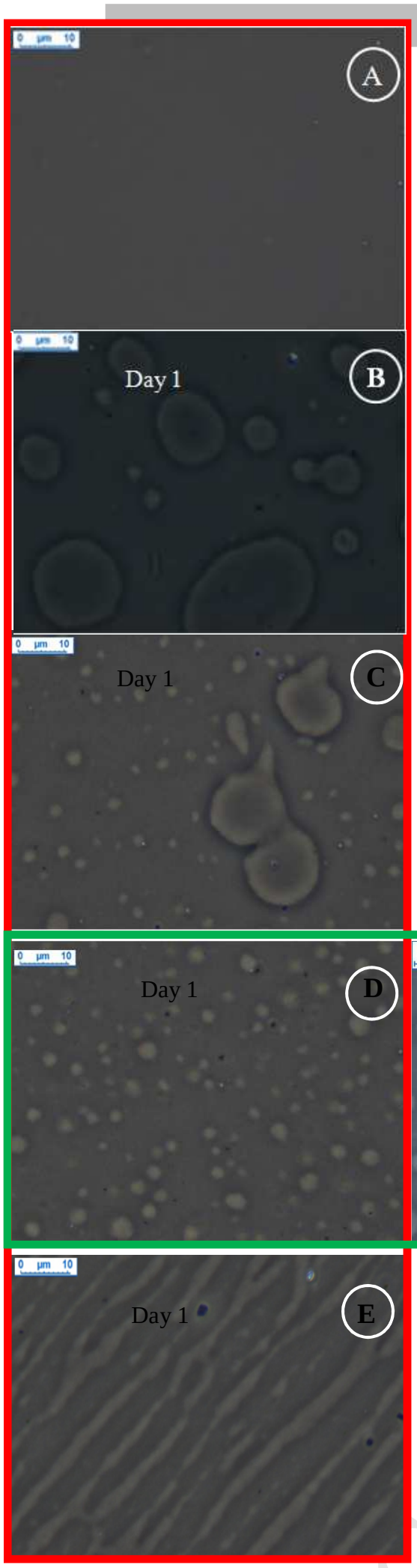
A
Day 1
B
Day 1
C
Day 1
D
Day 2
Day 4
Day 7
Day 1
E

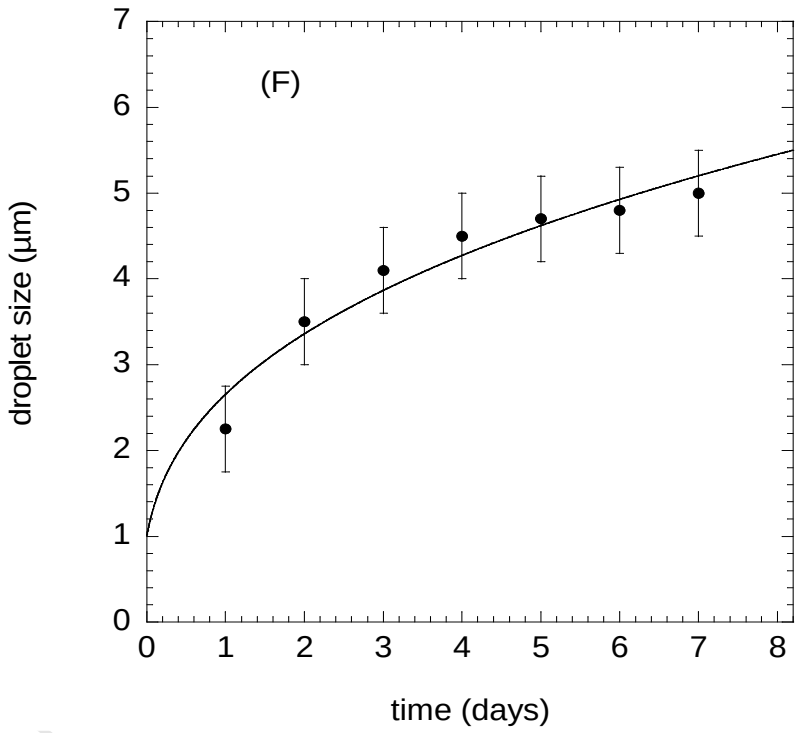
(F)
droplet size (µm)
time (days)
0
1
2
3
4
5
6
7
8

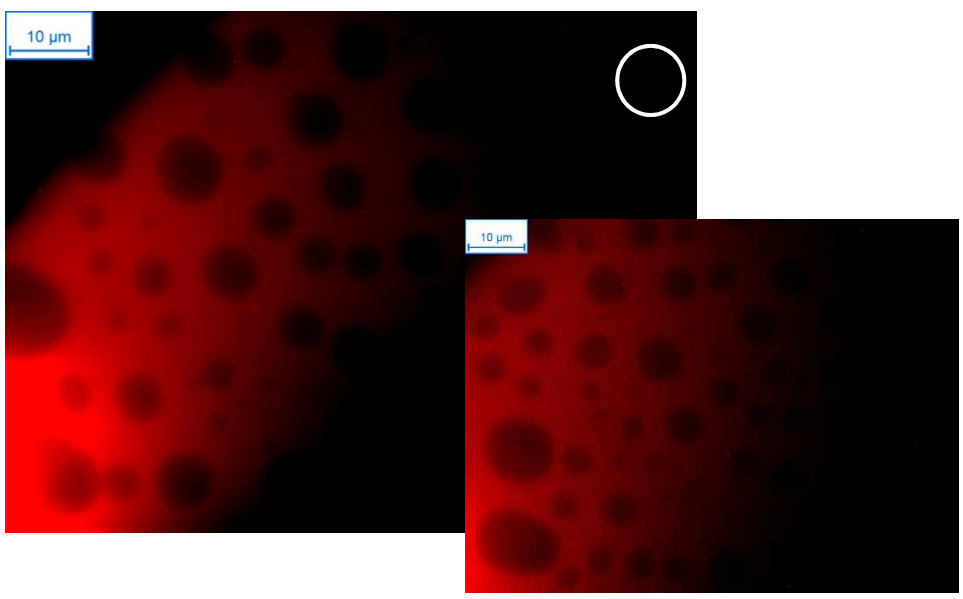

Figure 1.

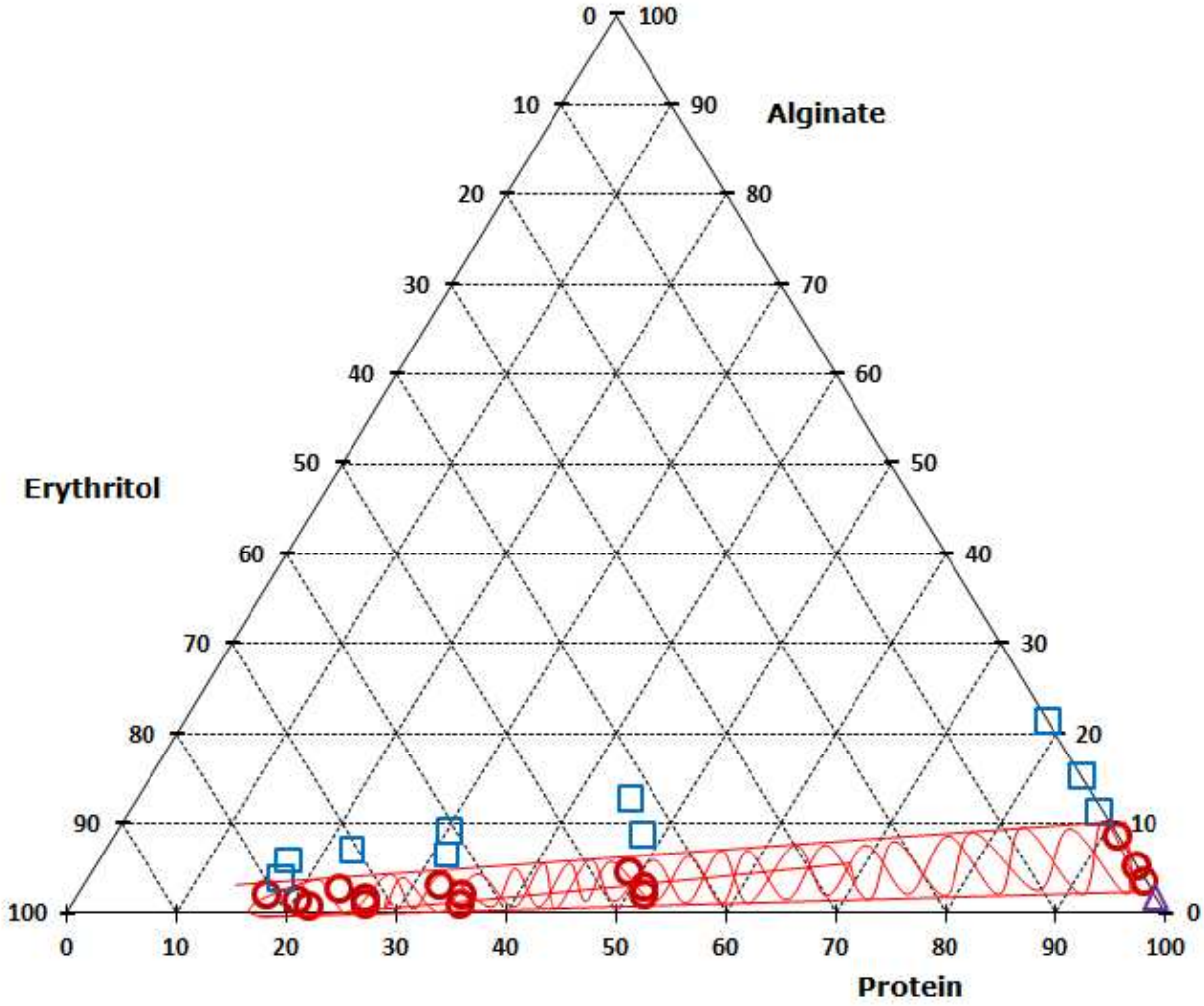

Figure 2.

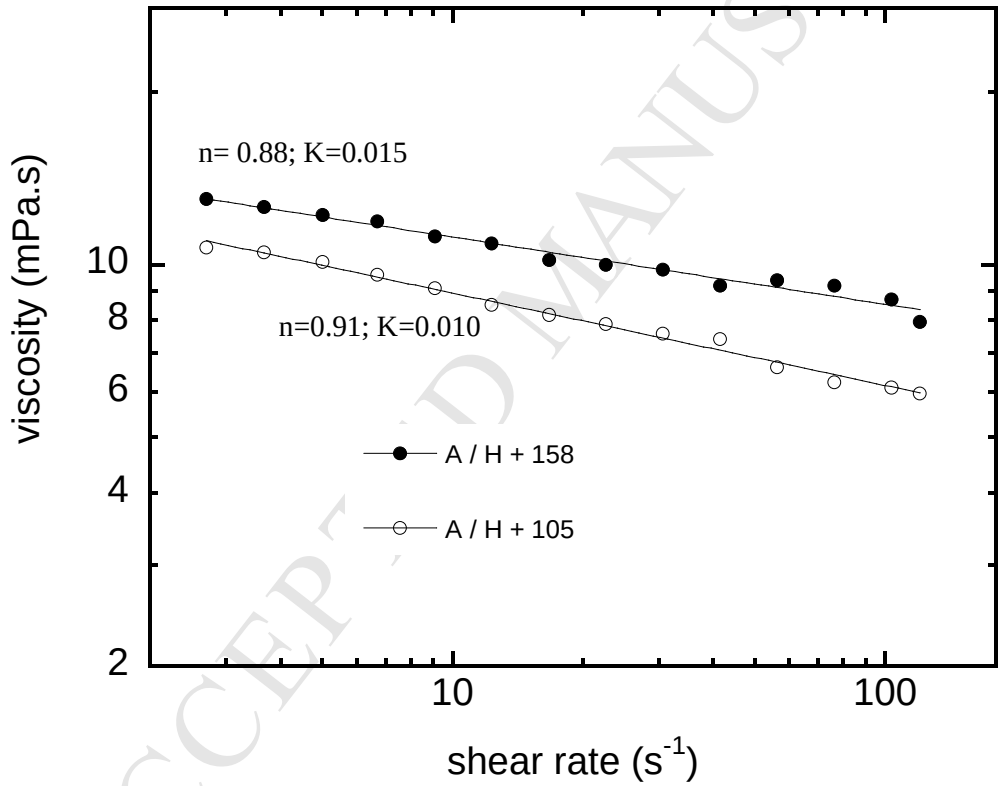

Figure 3.

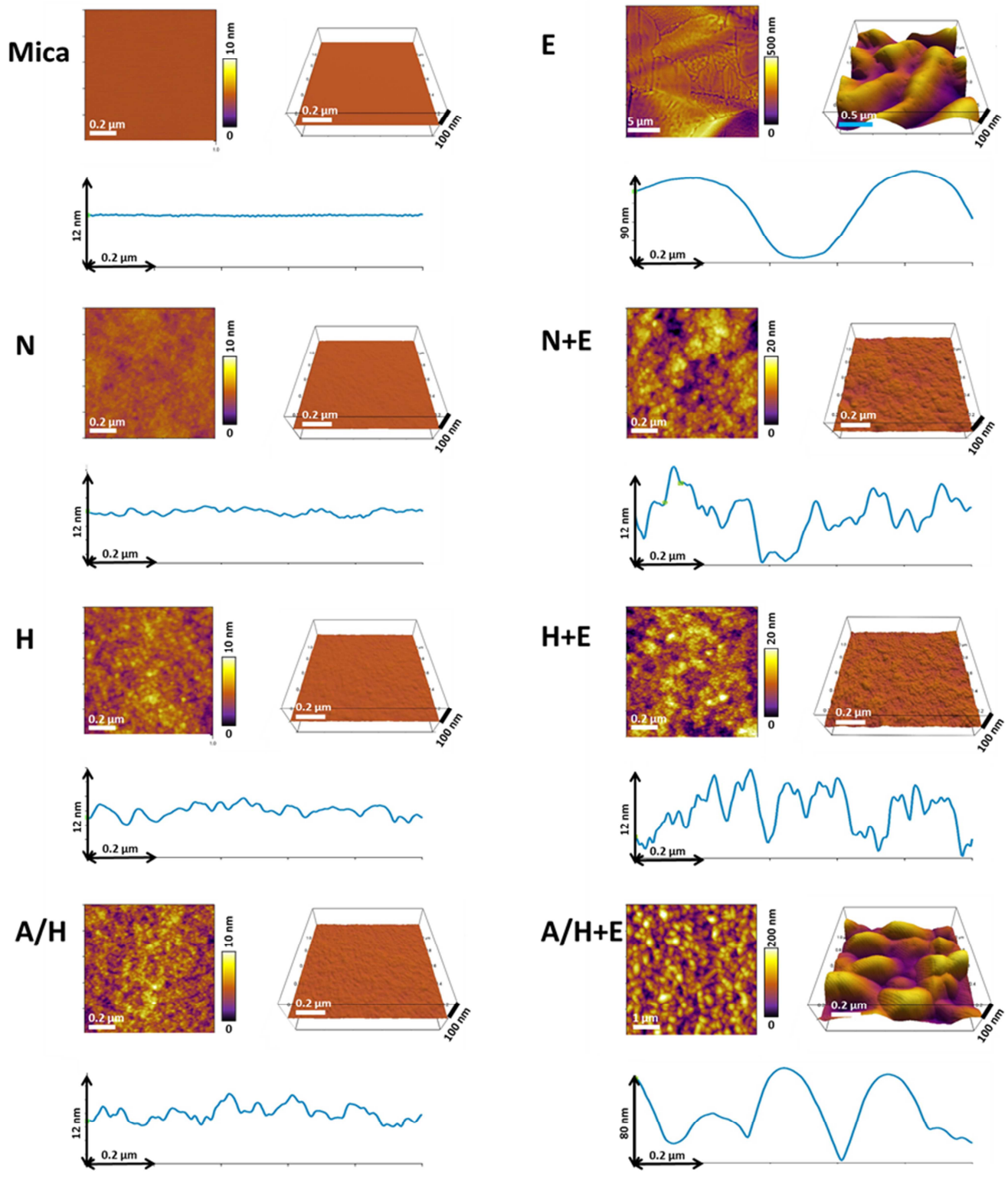
Mica
E
N
N+E
H
H+E
A/H
A/H+E
0.2 µm
5 µm
0.5 µm
100 nm
10 nm
500 nm
20 nm
200 nm
0
12 nm
90 nm
80 nm

Figure 4.

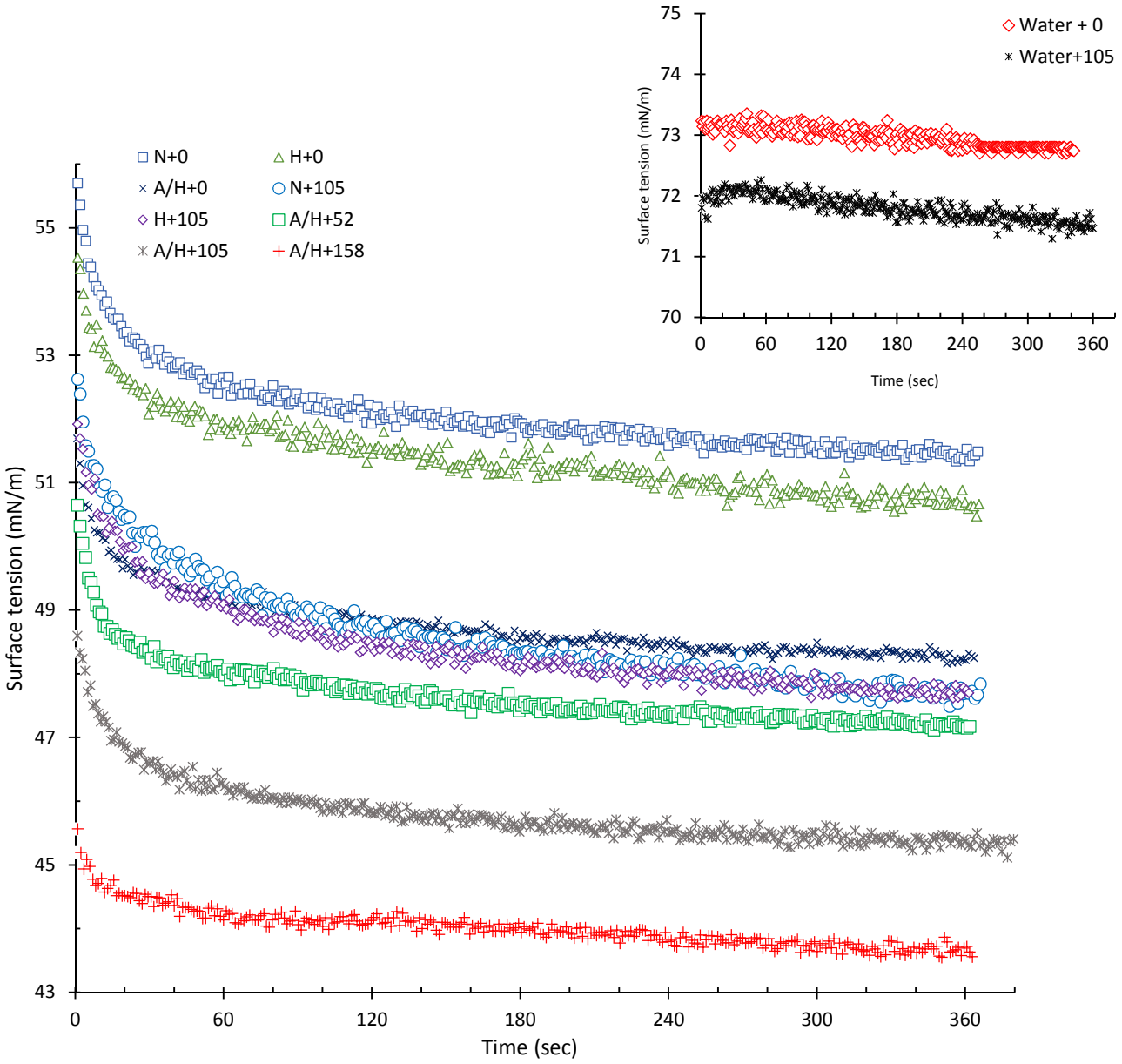
N+0
H+0
A/H+0
N+105
H+105
A/H+52
A/H+105
A/H+158
Surface tension (mN/m)
Time (sec)
Water + 0
Water+105
Surface tension (mN/m)
Time (sec)

Figure 5.

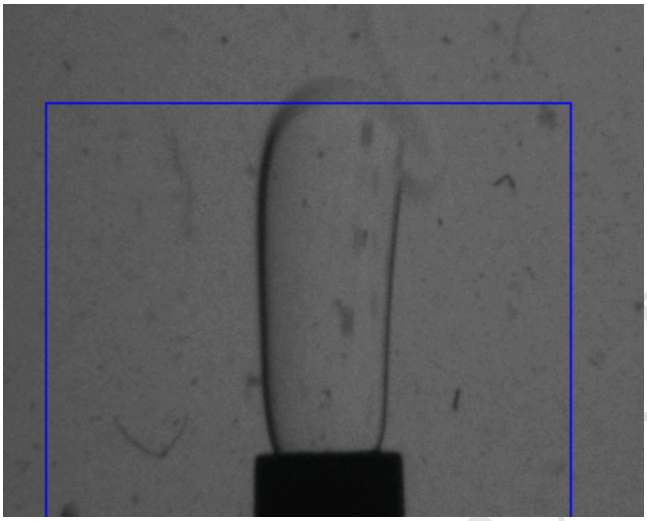

Figure 6.